JOURNAL OF AIRCRAFT
Vol. 37, No. 1, January–February 2000

Stiffener Shape Design to Minimize Interior Noise

S. P. Engelstad*
Lockheed Martin Aeronautical Systems, Marietta, Georgia 30063-0648
K. A. Cunefare†
Georgia Institute of Technology, Atlanta, Georgia 30332-0405
E. A. Powell‡
Lockheed Martin Aeronautical Systems, Marietta, Georgia 30063-0648
and
V. Biesel§
Georgia Institute of Technology, Atlanta, Georgia 30332-0405

Results of a research program to develop computational methods to minimize noise transmission into aircraft fuselage interiors are discussed. A design tool to perform a constrained optimization of the acoustic environment within a vibrating structure is developed utilizing finite element methods and boundary element methods (FEM/BEM), and its application to aircraft cabin noise problems is studied. The results of a study to optimize the cross section shapes of frames and stringers of an idealized aircraftlike stiffened cylinder are reviewed. The structure is optimized for minimum noise at specified points in the interior, as a result of a single frequency (tonal) exterior acoustic disturbance. For the cylinder and excitation frequency studied, it has been found that spatially varying the stiffener sizes over the cylinder is more important than optimizing the shape of the cross sections. Because FEM/BEM methods are only reliable for lower frequencies, the problems studied are applicable to low-frequency tonal noise such as seen in turboprop aircraft.

Nomenclature

$\boldsymbol{b}$	= design variable vector
$\boldsymbol{b}_L$, $\boldsymbol{b}_U$	= vectors of lower and upper bounds
$F(\boldsymbol{b})$	= objective function
f_0	= initial value of objective function
$p_i(\boldsymbol{b})$	= complex acoustic pressure at node i
S	= scale factor design variable
v	= normal velocity of shell structure, or acoustic velocity at shell wall
W	= structural weight
$W_{\max}$	= constrained maximum weight
x_i, y_i	= coordinate design variables at node i

Introduction

THIS paper presents the results of an optimization study to shape and size the stiffener cross sections (frames and stringers) of a stiffened cylinder. The optimization problem is formulated to minimize the interior noise environment subject to constraints on the structural weight of the cylinder. The cylinder is considered to be excited by an external noise source, modeled here as a monopole. Geometric points on the stiffener cross sections, as well as overall cross section sizing (scale) factors, are considered as design variables. Although the overall dimensions and stiffening characteristics of the cylinder are realistic in comparison to aircraft structure, the many variations and details that exist in a real aircraft have been eliminated and reduced to a cylinder segment. Thus, the model size is considerably smaller for study purposes. Future research will apply the algorithm to a real aircraft structure.

The need to improve the interior noise environment in new commercial aircraft is on the rise. Many techniques are utilized to reduce interior noise, all of which fall into the two broad categories of active and passive noise control.[1,2] The solution selected is highly dependent on the noise sources and, thus, on the resultant characteristics of the acoustic spectra. Much of today's commercial commuter air traffic is dominated by turboprop aircraft. The acoustic spectra of turboprops is characterized by low-frequency deterministic tones. Active noise control methods are being studied as one solution to this problem, and passive noise control is another possibility. The particular method of passive noise control considered in this work involves the inclusion of acoustic considerations into the structural design process. In the past, acoustic considerations have been included very late in the design process. In fact, many questions relating structural details such as stiffener/skin design to interior noise spectra could not be answered. With today's rapidly increasing computer speeds and efficient numerical methods to model the structural and acoustic media, it is possible to confront these low-frequency acoustic problems through optimization techniques.

The use of numerical optimization methods to design passive noise control into the structure is a form of multidisciplinary design optimization (MDO).[3] Several disciplines are involved in this problem, including exterior and interior acoustics, structural dynamics, static stress, and structural buckling. The context of the MDO problem in this work involves the minimization of acoustic levels, subject to weight constraints on the structure. For a more comprehensive review of the multidisciplinary design process, the reader is referred to an earlier paper by the authors.[4]

Although the literature in the parent category of MDO is quite rich, examples of structural acoustic optimization are not nearly as abundant. Some recent work that seeks to integrate acoustic considerations into the design optimization process includes those of Naghshineh and Koopmann[5] and Lamancusa.[6] Some examples of the use of structural acoustic optimization in industry have also appeared.[7–9] All of the latter citations are computational in nature, involving automation of the design optimization process. The

Presented as Paper 97-1620 at the AIAA/CEAS 3rd Aeroacoustics Conference, Atlanta, GA, 12–14 May 1997; received 26 April 1998; revision received 15 December 1998; accepted for publication 4 June 1999.

*Engineering Specialist Senior, Department 73-C2, 86 South Cobb Drive. Senior Member AIAA.
†Assistant Professor, George W. Woodruff School of Mechanical Engineering. Member AIAA.
‡Engineering Specialist Senior, Department 73-47, 86 South Cobb Drive. Senior Member AIAA.
§Research Associate, George W. Woodruff School of Mechanical Engineering.

present work is part of an ongoing research program to develop and validate a robust computational tool to minimize noise transmission into stiffened cylinders through the modification of the structural design.[4,10,11] Existing analysis tools have been utilized to solve the coupled structural acoustic problem, and a UNIX shell script maintains control and coordinates the iterative design process, integrating the programs. The present study is an application of this tool, in which the stiffener cross section dimensions and overall sizing is modified to achieve the improved interior noise environment.

The following section introduces the structural acoustic equations used and discusses the structural modeling assumptions. Next, the computational algorithm is introduced, followed by the optimization problem formulation. The subsequent sections describe the stiffened cylinder geometry and model and present results of the beam cross section shape optimization.

Structural Acoustic Equations

The structural acoustic problem involves a solution of the linear harmonic structural dynamics equations coupled with the linear acoustic wave equation. For the structural problem, the standard assumption of a steady solution to a harmonic loading results in the standard frequency-domain structural dynamics equations. The finite element method (FEM) is used for the structural analyses. For the acoustic problem, the governing equation is the Helmholtz equation, the time harmonic case of the linear wave equation. The acoustic boundary element method (BEM) is used for the required interior and exteror acoustic analyses. At present, the acoustic analysis is uncoupled, meaning that the vibration of the structure is not considered to be affected by the bounding acoustic medium.

The structure modeled is a stiffened circular shell. The finite element solution can be obtained by using linear 4-node plate elements for both the shell skin and the frame and stringer stiffeners or by using plates for the skin with beam elements for the stiffeners. The plate/beam element solution does an adequate job of predicting structural modes whose wavelengths are longer than the separation distance between stiffening elements. However, once the modal wavelengths are shorter than the subpanels formed between the stiffening elements, the beam elements are not adequate. Because they are line elements, the footprint formed by these elements on the shell results in subpanels that are effectively larger than in reality. To capture the subpanel modes, plate elements are also required for the stiffeners, which requires considerably more degrees of freedom.

We chose to use the plate/beam modeling technique because we are interested in low-frequency structural modes that are global in nature (long in wavelength) and, thus, couple very well with the internal acoustic airspace. In addition, the structure was assumed to be a bare skin, and thus no acoustic treatment was present in the model.

Algorithm Structure

We implement the optimization algorithm by integrating a number of standalone codes, with data exchange and process control coordinated by a UNIX shell script. Figure 1 is a flowchart showing the structure of the script's algorithm. The principal programs are a public domain optimizer CONMIN, a structural commercial FEM program, and an acoustic commercial BEM program. CONMIN is the optimizer that uses the modified method of feasible directions algorithm to optimize a single objective function subject to inequality constraints and side constraints on the design variables. Structural analyses are performed with the structural FEM program. The external and internal acoustic analyses of the cylinder are performed using the boundary element code.

Five other programs, BEAMSHPE, the mesh routine, the weight translator, the boundary condition (BC) translator, and the chain rule routine are supporting codes for the main programs. The meshing program and BEAMSHPE generate a beam cross section mesh and solve for beam section property equations, respectively. These two codes will be discussed more in depth in later sections. The weight translator extracts the total cylinder weight and weight sensitivities from the finite element output. The weight sensitivities

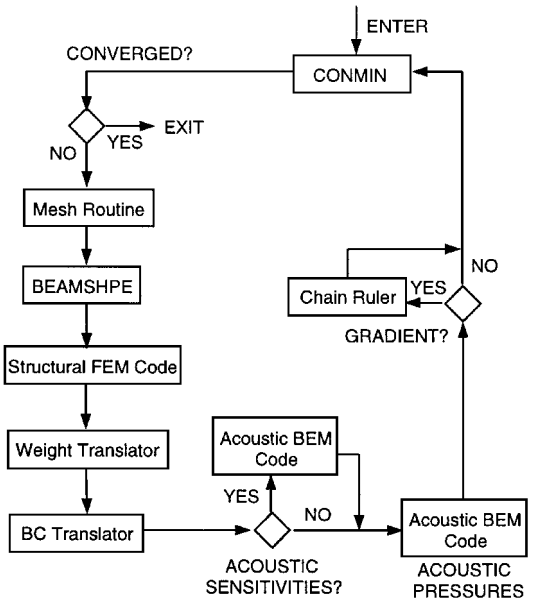

Fig. 1 Flowchart of design tool algorithm logic.

are the change in weight due to a change in a design variable. The BC program translates surface velocities from the finite element code into the boundary element input dataset as velocity BCs. The chain rule program combines structural design sensitivities from the structural and acoustics codes using the chain rule.

Optimization Problem Formulation

The optimization problem we pose here is straightforward: the minimization of the sum of the pressure magnitudes squared at a number of observation points within the cylinder. We impose a constraint on the weight of the cylinder, as well as upper and lower bounds on the design variables. We express this optimization problem as follows.

Minimize

$$F(\boldsymbol{b}) = \sum_{i=1}^{\text{NDRN}} \frac{|p_i(\boldsymbol{b})|^2}{f_0} = \sum_{i=1}^{\text{NDRN}} \frac{p_i(\boldsymbol{b})\, p_i^*(\boldsymbol{b})}{f_0} \tag{1}$$

subject to

$$[W(\boldsymbol{b})/W_{\max}] - 1 \leq 0 \tag{2}$$

$$\boldsymbol{b}_L \leq \boldsymbol{b} \leq \boldsymbol{b}_U \tag{3}$$

where $p_i(\boldsymbol{b})$ is the acoustic pressure at the ith point within the volume, NDRN is the number of data recovery nodes in the acoustic model, W is the total weight of the cylinder, and $W_{\max}$ is a user-specified maximum weight. The objective function is scaled by f_0, the value of the objective at the initial design state. Lower and upper bounds on the design variables are represented by $\boldsymbol{b}_L$ and $\boldsymbol{b}_U$, respectively.

The optimization algorithm requires gradients of the objective function and the weight constraint with respect to the design variables. The gradients of the objective are

$$\frac{\partial F}{\partial b_j} = \frac{2}{f_0} \sum_{i=1}^{\text{NDRN}} \text{Re}\left(p_i^* \frac{\partial p_i}{\partial b_j} \right) = \frac{2}{f_0} \sum_{i=1}^{\text{NDRN}} \text{Re}\left(p_i^* \frac{\partial p_i}{\partial v} \frac{\partial v}{\partial b_j} \right) \tag{4}$$

As a consequence of the coupled structural acoustic problem, we have used the chain rule for the derivative in Eq. (4). The gradient of the weight constraint is straightforward. We generate each of the derivatives in Eq. (4), as well as the weight sensitivity, using separate computational codes: $\partial p_i / \partial v$ by the acoustic BEM code and $\partial v / \partial \boldsymbol{b}$ and $\partial W / \partial \boldsymbol{b}$ by the structural FEM code.

Stiffened Cylinder Description

A stiffened uniform thickness cylinder, clamped at both ends is investigated to represent a fuselage structure. The excitation is a single tone exterior monopole source on one side of the fuselage, chosen to represent a propeller source. The cylinder geometry and excitation were modeled after that of the NASA composite test cylinder.[1] Figure 2 shows the structural FEM. There were 800 quad4 linear plate elements and 460 linear beam elements in this model. A cylindrical coordinate system (r, θ, x) is used with the origin in the center of the clamped end and with the x axis along the length of the cylinder. Because of the selection to study only symmetric modal response, only one-quarter of the cylinder is modeled ($0 \leq x \leq L/2$, $0 \leq \theta \leq \pi$). A direct frequency response solution is used to compute the structural velocity response. Structural damping at 1% of critical is applied to the cylinder.

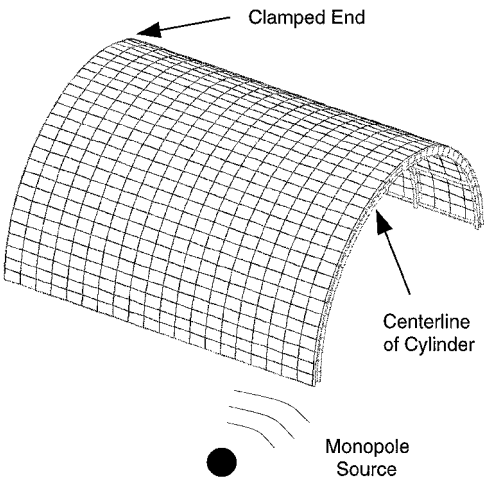

Fig. 2 Finite element structural model of stiffened cylinder.

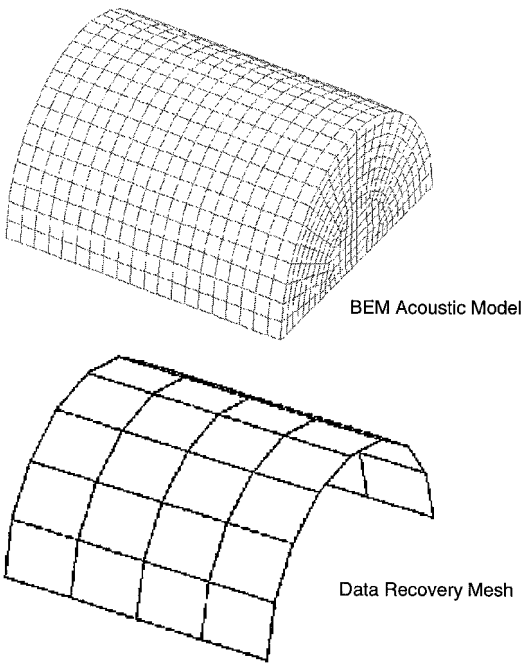

Fig. 3 Boundary element acoustic model and data recovery mesh.

The primary exterior acoustic field is due to a single monopole source at $x/L = 0.5$ and at a radial distance of $1.20R$, where R is the radius of the shell. Because an uncoupled structural acoustic formulation is utilized, the exterior and interior acoustic problems are solved separately, using an indirect BEM (variational) formulation. Thus, prior to optimization, the exterior acoustic problem is solved to determine the blocked pressure due to the monopole on the outside of the cylinder. This pressure is integrated to produce the external loading of the FEM model, and because a single analysis frequency is maintained, this loading remains constant throughout the optimization. The FEM structural and BEM interior acoustic responses are computed repeatedly in the optimization process.

Figure 3 shows the BEM boundary mesh and data recovery interior mesh. The boundary mesh density was set to handle the wavelengths appropriate for an analysis frequency of 250 Hz or less and utilized 1544 linear quad4 surface elements. The data recovery mesh is concentric with the structural model at a radial distance of $0.89R$ and was modeled using 45 points.

Single Frequency Beam Shape Optimization

As already discussed, the optimization is performed at a single frequency that for this case has been selected to be on resonance with a structural natural mode. The reason for this selection is the natural frequencies correspond to the peaks in any spectrum, and this optimization technique is designed to reduce the peaks, thereby reducing the overall spectrum. We have also shown in other work that even when we begin with an off-resonance starting point, the algorithm still tends to locate similar optimal designs as found when we begin on-resonance.[11] In later work we plan to discuss multifrequency optimization in which we reduce all of the peaks in a prescribed frequency band and at each iteration recompute the structural and acoustic natural modes and optimize, always following the peaks in the bandwidth. This is called peak tracking. In this example, single frequency optimization is performed, and we begin on a resonance of the structure. The shape of the structural natural mode is shown in Fig. 4, which for this structure had a frequency of 140.8 Hz. This frequency was the constant excitation frequency of the optimization.

To perform shape optimization of stiffeners modeled using beam elements, it is necessary to know the area A; inertias I_x, I_y, and I_{xy} about the cross section X, Y axes; the torsion constant J; and the centroidal and shear center locations. Because we are using the method of feasible directions to do the optimization, we also need the sensitivity derivatives of the responses with respect to the design variables. These properties and derivatives must be evaluated when requested by the optimizer at each iteration. The structural FEM code has the capability of accepting properties such as A, I_x, I_y, I_{xy}, J, etc., in equation form as they would be programmed in FORTRAN. To compute the equations, a separate finite element code was written to integrate these area properties over the cross

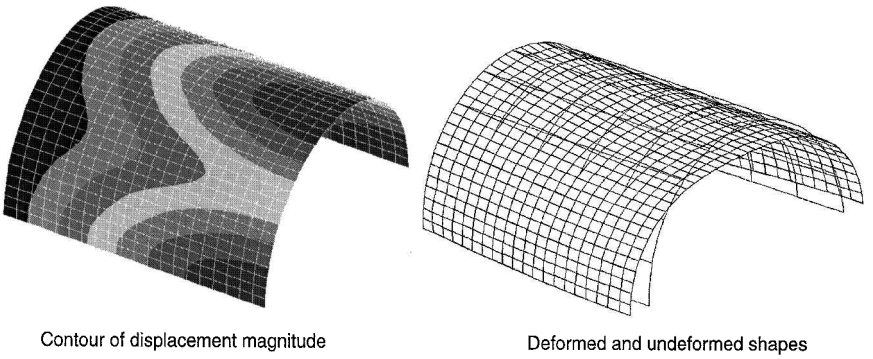

Fig. 4 Structural natural model shape.

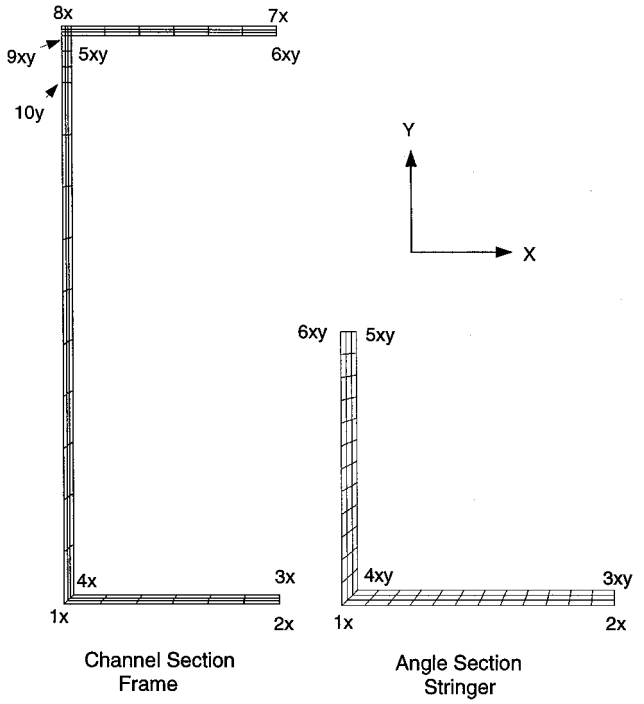

Fig. 5 Frame and stringer cross section shapes and finite element discretization.

sections as they exist at each iteration. This standalone finite element code was written such that it did not output the values of the properties (A, I_x, I_y, I_{xy}, J, etc.), but did output the property equations as a function of certain prescribed X, Y coordinates of the mesh for that cross section. These X, Y coordinates correspond to the design variables of the cross section. Having coordinates as design variables allows one to alter the shape of the cross section.

Figure 5 shows the frame and stringer cross section shapes, along with the finite element discretization. Shown here are a channel section for the frame and an angle section for the stringer (this is case I; case II will be discussed later). The labeled points indicate the design variable locations, with subscript x corresponding to an X-direction design variable and subscript y to a Y-direction design variable. Note that some nodes only have an x subscript, some a y subscript, whereas others have an x, y subscript. Each x or y at a node indicates a separate design variable, with the direction indicating the degree of freedom. By specifying only one of the coordinate directions at a node, the shape is, thus, constrained only in that direction. This is a way of limiting or constraining the design.

Note that at each iteration in which the FEM/BEM solution was run, the cross section finite element code had to be run to evaluate the property equations. The cross section code, called BEAMSHPE, requires finite element discretization of the cross section shapes. This was performed using an automated meshing code. The meshing code was run prior to each BEAMSHPE execution. Note that a coarse finite element discretization was found adequate to evaluate the area properties accurately.

At this stage we can vary the coordinates of the two cross sections at every iteration due to changes in x_i, y_i coordinate design variables. To vary independently the cross sections of the 5 frames and 11 stringers in the model, we would require 175 coordinate design variables. This would be excessive and is really not necessary. Instead we introduced design variables that basically were scale factors of each parent cross section, which are multiplied by each coordinate equally to scale uniformly the section up or down. The relationship between a property value A (area), the scale factors S, and design variable coordinates x_i and y_i is

$$A(S, x_i, y_i) = g(S \times x_i, S \times y_i) \tag{5}$$

where g represents the equation for the area in terms of coordinates of x_i and y_i. A separate scale factor was applied to each frame and stringer in the model. Because there were 5 frames and 11 stringers, a total of 16 scale factor design variables were required. Adding these to the 23 coordinate design variables for the parent cross sections, we had a total of 39 design variables.

When performing optimization using any gradient search method, the starting point in the design space is very important. It is ususally necessary to evaluate many starting points to locate approximately a global minimum. In the case at hand, we have a mixture of coordinate design variables and scale factor design variables. Depending on the initial values of the scale factors relative to the coordinates, the gradients of scale factors or coordinates can be dominant. As it is possible to adjust the coordinate values with the scale factors and still have the same property starting values, the coordinates and scale factors were adjusted so that the initial gradients for scale factors vs coordinates were comparable in magnitude for the same values of the properties. This was done so as not to bias the design toward cross section shape change vs a spatial scale change. These starting values were varied for several different optimization runs, to test for sensitivity to starting point.

Each design variable, whether it is a scale factor or a coordinate, has upper and lower bounds. These were allowed to be quite generous, except for the case where a coordinate change may cause a line of the outline of the area to pass over another line, thus resulting in a negative area or inertia property. These bounds were used to control and maintain realistic values. In addition to the design variable bounds, a weight constraint was placed on the total cylinder weight such that the initial weight of the entire stiffened cylinder was not exceeded.

Figure 6 shows the changes in the acoustic objective and weight over the history of the iterations. The objective is given in pressure squared normalized by the initial pressure squared, and the weight is normalized by the initial weight. The global objective was reduced by 8.6 dB, and the weight, which was constrained to not exceed the initial weight, was actually reduced by 5%. Also note that each design iteration required approximately 15 CPU min on an SGI Power Indigo II workstation, with a total of 19 CPU h.

In Fig. 7, the before and after optimization parent cross section shapes are presented. Note that the sections have been greatly enlarged for clarity. For both cases, dramatic changes in the shape of the cross sections were not found. Typically, thinning down of the sections, maintaining inertia while reducing weight, is the trend for the channel. Attempts were made to allow the channel (frame) section the freedom to develop another leg at the top (away from the attachment to the shell), and only a bump is noticeable. It is evident that the angle's stiffness and mass are reduced considerably. Note that the thinner sections are still multiplied by the scaling factors.

The dominant change in the stiffener design tended to be in the scaling variation from stiffener to stiffener over the cylinder, represented by the scale factor design variables. Figure 8 shows this

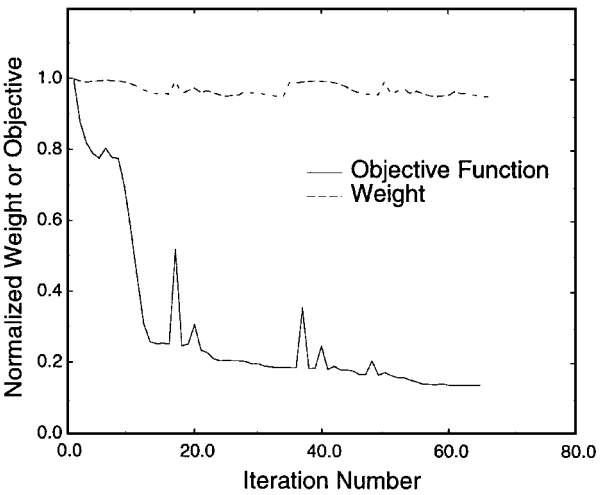

Fig. 6 Objective function and weight iteration history.

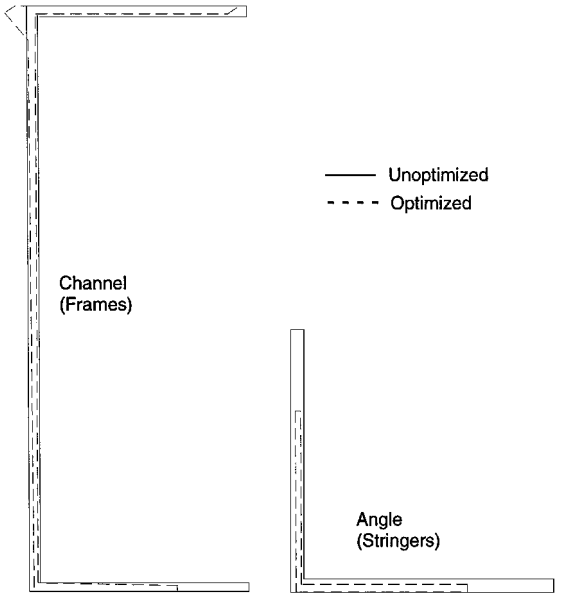

Fig. 7 Before and after optimization cross section shapes.

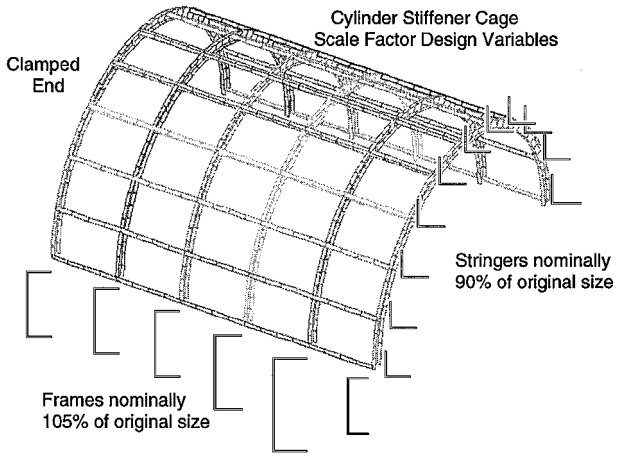

Fig. 8 Relative changes in stiffener size over the cylinder, case I.

trend. The scale factors are magnified and multiplied by the parent sections to show the relative changes in size over the cylinder. In general, the frame relative size changes can be seen, but not much visible variation is evident in the stringers.

Figure 9 shows a plot of the vibration natural modes of the stiffened cylinder before and after optimization and the acoustic natural modes of the cylindrical cavity. It is evident that the modal density of the stiffened cylinder within ±50 Hz of the excitation frequency is quite low, as only 3–4 modes are present in this range. It is also seen that the (2, 1) structural mode at 140.8 Hz (before) and 144.5 Hz (after) forces the off-resonance response of the (2, 0) and (2, 2) acoustic modes at 197.2 and 218.0 Hz, respectively. Close inspection of the (2, 1) structural mode shape before and after optimization shows no discernable differences. Thus, for this case of single frequency optimization, the reduction in acoustic response is due to frequency mismatch of the optimized structural (2, 1) mode at 144.5 Hz with the excitation frequency of 140.8 Hz. As the weight constraint allowed no weight increase, the optimizer redistributed the stiffness, which resulted in the same overall structural mode but at a different frequency.

The results of only a single case study has been presented (case I). Many starting points, which consist of perturbations of the design variable space, were run for this case. Similar end designs were discovered for all of these starting points. A second case study (case II) was studied in which the initial stringer cross section was a different design. For brevity, the details of this cross section will not be

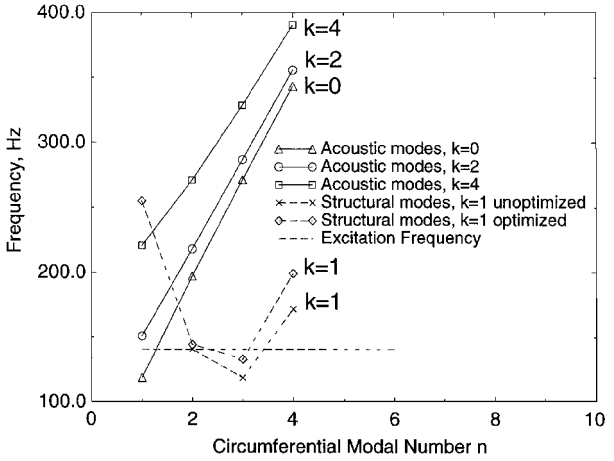

Fig. 9 Stiffened cylinder and cavity natural modes, k = axial mode number.

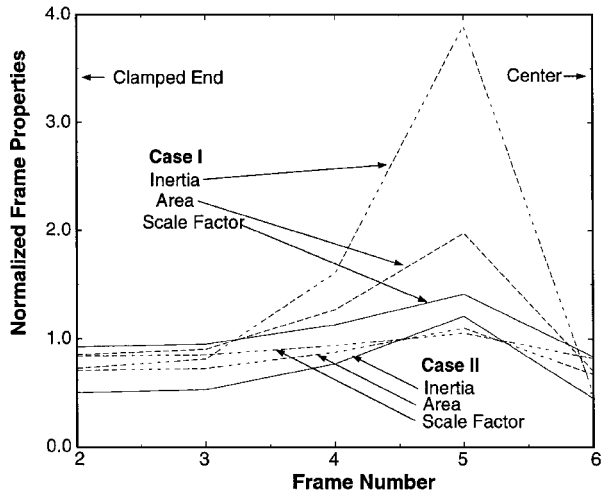

Fig. 10a Normalized frame cross section properties over the cylinder; frame 1 is at the clamped end and was not a design variable.

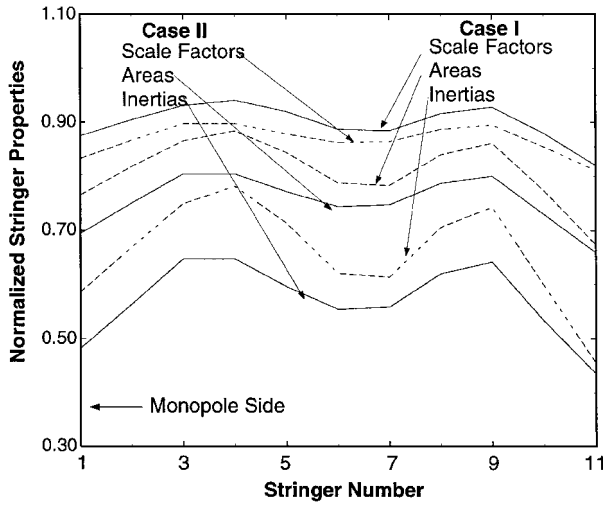

Fig. 10b Normalized stringer cross section properties over the cylinder.

discussed, but it is another potential section design. Case II is introduced to enrich the following discussion by showing the variation in the results for two cases.

A plot of the scale factors over the surface of the cylinder is not a good indicator of how they will affect the dynamic response of the cylinder or the acoustic response of the interior. Figures 10a and 10b contain plots of the cross section properties of the frames and stringers normalized with respect to the initial values prior to

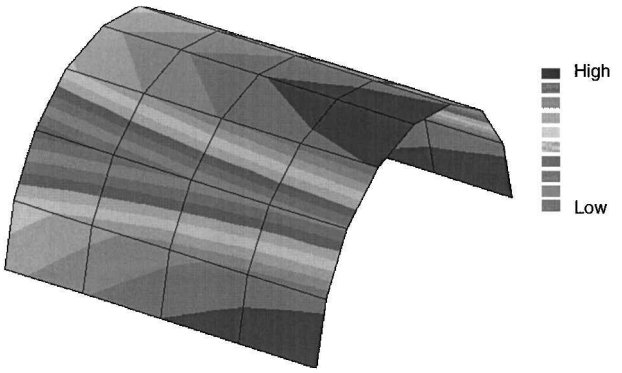

Fig. 11 Contour of relative acoustic response of data recovery mesh to the structural natural mode.

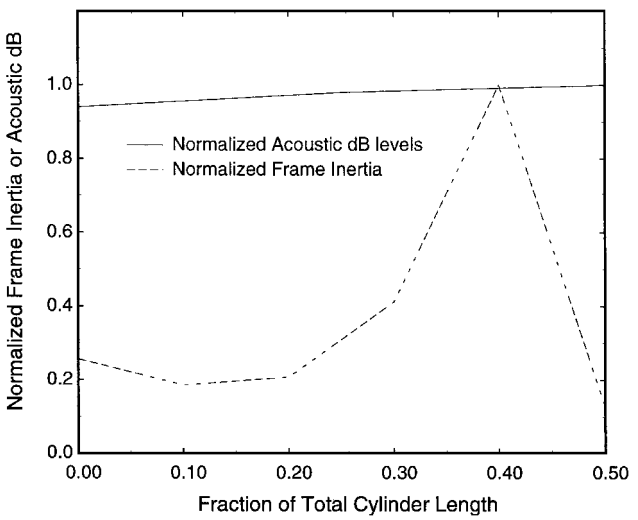

Fig. 12a Normalized acoustic response and normalized frame inertia properties over the cylinder length.

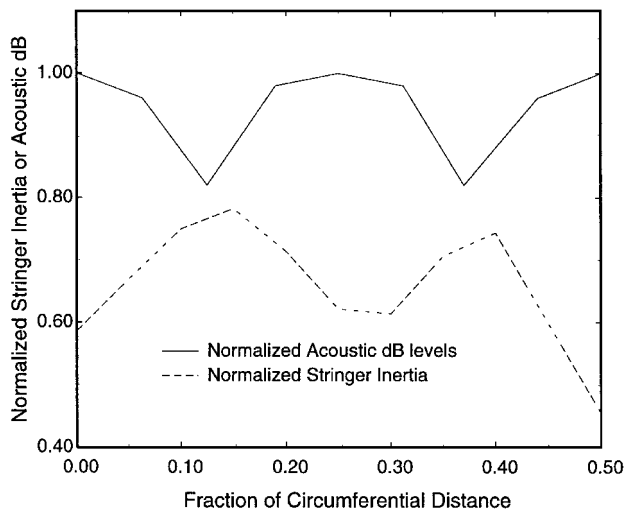

Fig. 12b Normalized acoustic response and normalized stringer inertia properties over the cylinder circumference.

the optimization. These properties include the scale factors, areas, and inertias (I_x, I_y, I_{xy}, and J). Note that the area changes are proportional to the square of the scale factors and the inertias to the 4th power of the scale factors. In Fig. 10, it is evident that small changes in scale factors result in large changes in inertias. It is the inertias that strongly affect the bending behavior of the shell and, thus, the acoustic response of the interior. In Fig. 10a, it is clear that the inertias are much larger for case I than in case II. In Fig. 10b, a sinusoidal variation in stiffness properties around the circumference is evident for both cases (this result has also been found in earlier work by the authors in which the same cylinder was optimized using shell element thicknesses as the design variables[11]). For case I, the stringers were nominally 90% of original size and for case II were 87% of original size. It is noted that similar trends were found for both cases.

Looking back at Fig. 4, this starting natural mode of the structure is a (2, 1) mode, that is, two sine waves in the circumferential direction and one-half sine wave in the longitudinal direction (recall that only half of the longitudinal and circumferential directions are modeled). Figure 11 is a contour of the relative magnitude of the acoustic response at the subject frequency to this structural mode. The dark regions correspond to the higher responses. The acoustic mode shapes have a two sine wave variation circumferentially and a $\cos(k\pi x/L)$ variation in the longitudinal direction, where $k = 0$ or 2 for these modes. In Figs. 12a and 12b, this same acoustic behavior is plotted in a normalized fashion along with the changes in inertias along the longitudinal and circumferential axes, respectively. The acoustic curves are the pressure squared acoustic objective normalized by the maximum level in the contour, and the inertias are normalized by the maximum intertia. The particular case displayed is that of case I. Case II has very similar trends. Focusing on Fig. 12a, which corresponds to the longitudinal direction, the acoustic variation is a slowly increasing function, whereas the inertia variation has a spike near but prior to the center. In Fig. 12b, the acoustic variation appears to be that of two full sine waves around the half-circumference[$\sin(k\pi x/L)$ where $n = 4$] because the pressure squared objective is plotted, and, thus, the negative part of the wave has become positive (the pressure is actually still an $n = 2$ wave). The stiffener inertia around the circumference is also an $n = 4$ sinusoidal distribution, except it is different in phase by 180 deg. It is evident that the optimal design for this case involves a harmonic circumferential spatial variation in stiffener bending inertia around the circumference, with a strong phase relationship to the acoustic natural mode shape.

Conclusions

The results of this study indicate that it is possible to reduce the interior noise of an aircraftlike stiffened cylinder by tailoring the stiffener characteristics. For the particular cylinder and excitation frequency considered, we found that tailoring the stiffener section sizes from stiffener to stiffener was more important than optimizing the shape of the cross section. The optimization tended to alter the stiffening characteristics in a harmonic fashion from stiffener to stiffener. Small changes in stiffener sizes result in large changes in inertias that strongly affects the bending behavior of the shell. The shaping of the sections was dominated by thinning of the sections where stiffness/mass was not required. This result made it possible to vary the stiffening and mass properties, while maintaining relatively the same or slightly less overall weight.

We do not propose that these physical results can be universally applied to any airframe structure. We argue that the results indicate that much more can be done to improve the interior noise quality within an aircraft fuselage in the low-frequency range, using passive structural design techniques that tailor the stiffening design. Of course, this study was limited to a single frequency excitation, and work is in progress to extend it to multifrequency optimization.

Acknowledgments

The authors gratefully acknowledge the support of the Structural Acoustics Branch of NASA Langley Research Center under Contract NAS1-20102, with J. H. Robinson NASA Technical Monitor.

References

[1] Grosveld, F. W., Coats, T. J., Lester, H. C., and Silcox, R. J., "A Numerical Study of Active Structural Acoustic Control in a Stiffened, Double Wall Cylinder," *Proceedings of NOISE-CON 94*, National Conf. on Noise Control Engineering, Noise Control Foundation, Poughkeepsie, NY, 1994, pp. 403–408.

[2]Elliot, S., Nelson, P., Strothers, I., and Bocher, C., "In-Flight Experiments on the Active Control of Propeller-Induced Cabin Noise," AIAA Paper 89-1047, April 1989.

[3]Padula, S. L., "Progress in Multidisciplinary Design Optimization at NASA Langley," NASA TM 107754, July 1993.

[4]Crane, S. P., Cunefare, K. A., Engelstad S. P., and Powell, E. A., "A Comparison of Optimization Formulations for Design Minimization of Aircraft Interior Noise," AIAA Paper 96-1480, April 1996.

[5]Naghshineh, K., and Koopmann, G. H., "A Design Method for Achieving Weak Radiator Structures Using Active Vibration Control," *Journal of the Acoustical Society of America*, Vol. 92, No. 3, 1992, pp. 856–870.

[6]Lamancusa, J. S., "Numerical Optimization Techniques for Structural-Acoustic Design of Rectangular Panels," *Computers and Structures*, Vol. 48, No. 4, 1993, pp. 661–675.

[7]Müller, G., Tiefenthaler, P., and Imgrund, M., "Design Optimization with the Finite Element Program ANSYS," Software Systems for Structural Optimization, International Series of Numerical Mathematics, Vol. 110, Birkhäuser Verlag, Berlin, 1993.

[8]Yang, T. C., and Cheng, C. H., "Integrating and Automating Analysis and Optimization," Computers and Structures, Vol. 48, No. 6, 1993, pp. 1083–1106.

[9]Bråmå, T., "The Structural Optimization System OPTSYS," Software Systems for Structural Optimization, International Series of Numerical Mathematics, Vol. 110, Birkhäuser Verlag, Berlin, 1993.

[10]Engelstad, S. P., Cunefare, K. A., Crane, S., and Powell, E. A., "Optimization Strategies for Minimum Interior Noise and Weight Using FEM/BEM," *Proceedings of 1995 International Conference on Noise Control Engineering*, Noise Control Foundation, Poughkeepsie, NY, 1995, pp. 1205–1208.

[11]Cunefare, K. A., Crane, S. P., Engelstad, S. P., and Powell, E. A., "Design Minimization of Noise in Stiffened Cylinders Due to Tonal External Excitation," *Journal of Aircraft*, Vol. 36, No. 3, 1999, pp. 563–570.